# Thickness and cation control of conduction in nickelate heterostructures

X. Yang and O.K. Andersen

A hundred years after the discovery of superconductivity, no new superconductor has yet been found by *design*, but merely by chance, or by following empirical rules which the next discovery then proved to be of limited validity. The discoveries of the A15 compounds in the seventies, the cuprates in the eighties, $MgB_2$ in 2001, and the iron pnictides in 2008 all testify to this. Despite 25 years' intensive research, high-temperature superconductivity in the cuprates has not been understood and no superconductor with $T_c$ higher than 150 K has been found since 1993. This record-holding material is triple layer, pressurized $HgBa_2Ca_2Cu_3O_8$. Even in cases like $MgB_2$ where the superconductivity mechanism has been understood, this has not helped to design a better superconductor.

Recently, it has recently become possible to grow oxide heterostructures with great precision, specifically by pulsed laser deposition (PLD) or molecular beam epitaxy (MBE). This opens the possibility to produce materials with desired physical properties, for instance by manipulating the nearly localized 3*d*-electrons in transition metal oxides. This is becoming a major activity in our institute. Chaloupka and Khaliullin [1] speculated that by confining a single layer of $LaNiO_3$ with electronic configuration $d^7$ between layers of a lattice-matched, insulating perovskite such as $LaAlO_3$ or $LaGaO_3$, one might be able to force the Ni $3d\,(e_g)$ electron into the planar $x^2-y^2$ orbital as in the $d^9$ cuprates, and maybe in this way obtain high-temperature superconductivity.

Figure 1 illustrates the principle of this *confinement*: Bulk $LaNiO_3$ is a (pseudo)cubic, paramagnetic metal with electronic configuration Ni $3d^7$, i.e., with one electron in a doubly-degenerate $e_g$ band. Its two Wannier orbitals,

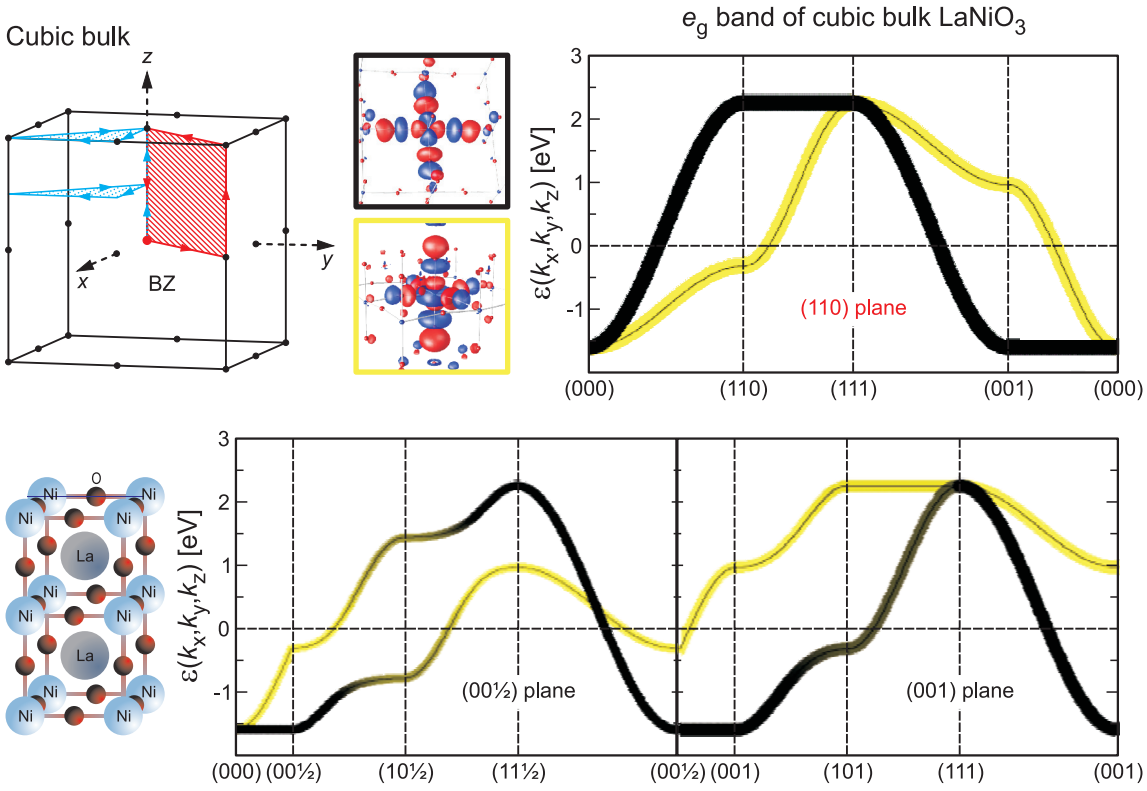


Figure 1: Brillouin zone, Ni $e_g$ Wannier orbitals ($x^2-y^2$ black, $3z^2-1$ yellow), $e_g$ energy band, and structure of cubic bulk $LaNiO_3$. The Fermi level is at 0 eV.

$x^2-y^2$ and $3z^2-1$, are shown respectively inside the black and yellow frames, and are seen to have antibonding $pd\sigma$ tails on the neighboring oxygens. Being formed from orbitals with respectively $|m|=2$ and 0, the two $e_g$ Bloch sums cannot hybridize when $\mathbf{k}$ is in a (110) plane, and it is therefore simple to understand the $e_g$ band structure along the red path in the cubic Brillouin zone (BZ). We see that the $x^2-y^2$ band disperses with $k_x$ and $k_y$, but *not* with $k_z$, and that the $3z^2-1$ band disperses *mainly* with $k_z$. At their common bottom, at (0,0,0), the bands have pure Ni $3d$ character, i.e., in the $\mathbf{k}=\mathbf{0}$ Bloch sums, the O $2p$ tails cancel. At their common top, at (1,1,1) $\frac{\pi}{a}$, the bands have *maximal* oxygen antibonding character.

Hence, the entire dispersion is due to hopping via oxygen. Shown in the second line of the figure are the bands along the blue paths in the BZ. Here, they hybridize as indicated by the mixed black and yellow colors. In this cubic bulk structure, the two $e_g$ orbitals are degenerate, e.g., the $x^2-y^2$ and $3z^2-1$ projected densities of states are identical, and so are the numbers of $x^2-y^2$ and $3z^2-1$ electrons obtained by integrating up to the Fermi level ($\equiv 0$).

However, substitution of every second $NiO_2$ layer by an 'insulating' $AlO_2$ layer, as shown on the left-hand side of Fig. 2, forces the Bloch waves to vanish near the insulating layers whereby the waves with $k_z \lesssim \frac{1}{2}\frac{\pi}{a}$ become forbidden. This changes the energy of the waves with $3z^2-1$ character, but not of those with $x^2-y^2$ character. One therefore expects the nearly 2D $e_g$ band of such a 1/1 heterostructure to look like the cubic band at some effective $k_z$-value, which depends on the scattering properties of the insulator and lies in the range between $\frac{1}{2}\frac{\pi}{a}$ and $\frac{\pi}{a}$, i.e., like those in the second line of Fig. 1, with the (000)-(00$\frac{1}{2}$) bit excluded. Figure 2 now shows that this holds surprisingly well. The band structures in Fig. 2 result from density-functional (GGA) calculations with structural optimization for two 1/1 heterostructures, $LaNiO_3/LaAlO_3$ and $LaNiO_3/YScO_3$ [2]. Like for the cubic case, the $e_g$ band has been colored according to its orbital character, but all bands are now included in order to show that the $e_g$ band is placed in a 2–3 eV gap above the Ni $t_{2g}$ and oxygen $p$ bands, and below the Ni $4s$, La or Dy $5d$, and Al $3sp$ or Sc $3d$ bands.

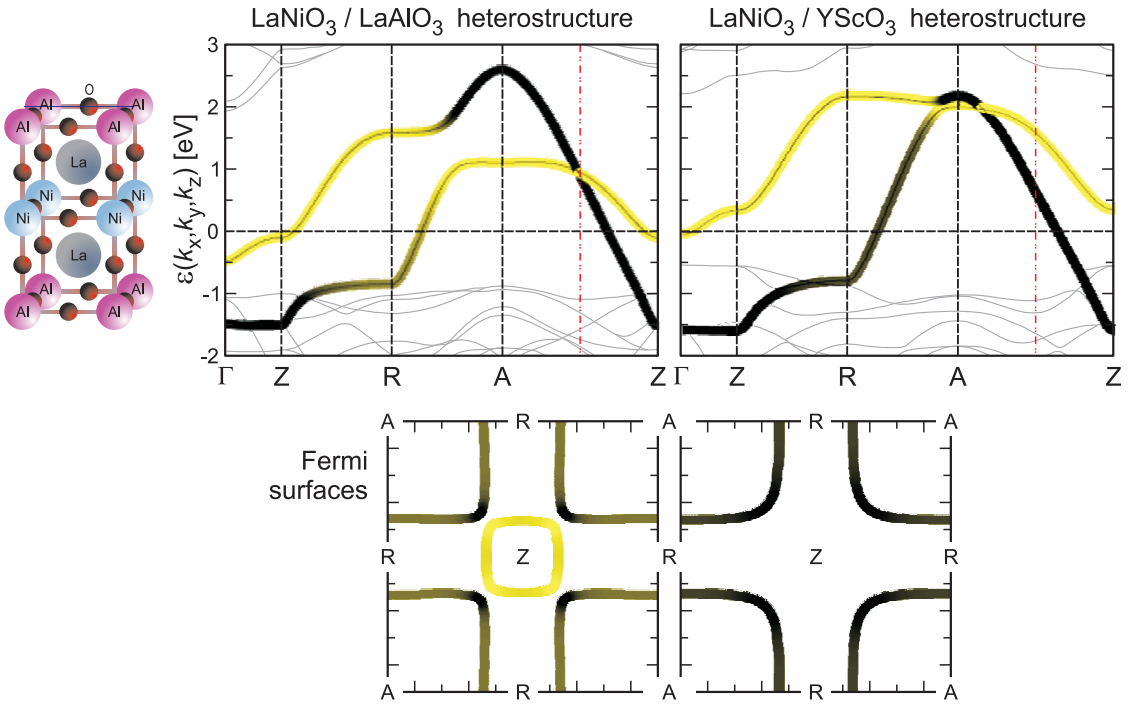


Figure 2: Structure, DFT energy bands, and Fermi surface of $LaNiO_3/LaAlO_3$ heterostructure. Similarly for the $LaNiO_3/YScO_3$ heterostructure. The bands are plotted along lines with the same horizontal projection as in the second line of Fig. 1 and with $k_z=\frac{\pi}{c}\sim\frac{\pi}{2a}$, except $\Gamma=(0,0,0)$. The red dot-dashed line is at $(k_x,k_y)=(\frac{1}{2},\frac{1}{2})\frac{\pi}{a}$. The Fermi surfaces are plotted in the $k_z=\frac{1}{2}\frac{\pi}{c}$ plane.

We see that the confinement in $LaNiO_3/LaAlO_3$ has pushed the bottom of the $(3z^2-1)$-like band up to 0.5 eV below the Fermi level, and in $LaNiO_3/YScO_3$ has even emptied this upper $e_g$ band.

Hence, the GGA Fermi surface of the aluminate has two sheets while that of the scandate has only one, and the latter is very similar in *shape* and *character* (predominantly $x^2-y^2$) to the ones in the cuprates with the highest $T_{c\,max}$ [2,3]. Also *Coulomb correlation* will tend to reduce the Fermi surface to one sheet [2], but the effect is smaller than the one seen in Fig. 2 which is obtained by change of cations.

Moving apical oxygen closer to Ni by the application of *tensile strain*, we have found to be inefficient in emptying the $(3z^2-1)$-like band in $LaNiO_3/LaAlO_3$ [2]. The reason is, that the bottom of the $3z^2-1$ band in the heterostructure has little oxygen character because for the cubic band, the oxygen character and thereby the strain dependence increases from *zero* at the bottom to a maximum at the top.

Adding *more insulating layers* helps a bit in emptying the upper band by diminishing the $k_z$-dispersion seen along ΓZ in Fig. 2. Adding more $NiO_2$ layers, or rather: *Failing to grow intact single* $NiO_2$*-layers*, should be *devastating* because interlayer hopping between $3z^2-1$ orbitals splits the $(3z^2-1)$-like bands by about 0.5 eV and thereby makes the lowest band dip below the Fermi level.

What determines the shape of the $(x^2-y^2)$-like Fermi-surface sheet is its hybridization with the *axial* $(m=0)$ *orbital* [3]. As was mentioned above, this hybridization vanishes for $k_x=k_y$ and is maximal near $(k_x,k_y)=(1,0)$ and $(0,1)\,\frac{\pi}{a}$ (R), where it pushes the energy of the saddle-point down. Hence, if we imagine continuing the trend seen in Fig. 2 by moving the energy of the axial orbital higher and higher above that of the $(x^2-y^2)$-orbital, the saddle-point would move up towards the center of that band, whereby the Fermi surface would turn by 45° around the $(1,1)\,\frac{\pi}{a}$ point (A). This shape is the one found for cuprates such as $La_2CuO_4$ with fairly low $T_{c\,max}$, while cuprates with high $T_{c\,max}$ have Fermi-surface sheets like the one calculated for $LaNiO_3/YScO_3$ and shown in the right-hand side of Fig. 2.

The upper parts of Fig. 3 now show schematically how the energy of the axial orbital is controlled in a nickelate heterostructure (left) and in a cuprate (right).

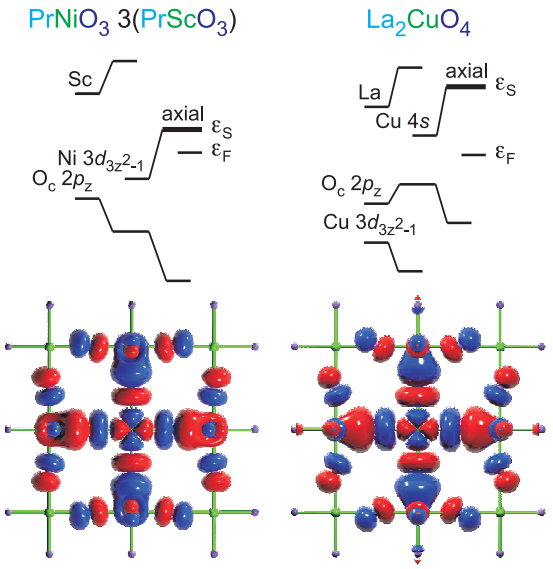


Figure 3: Comparison between nickelate and cuprate axial-orbital levels and conduction band Wannier functions.

In the nickelate, the axial orbital is the following linear combination of atomic orbitals: Ni $3d_{3z^2-1}$ antibonding to the two neighboring apical-oxygen $2p_z$ orbitals, each of which bond to their neighbor *cation* axial orbital, i.e., Al $3s\,3p_z$ or Sc $3d_{3z-1}$. We wish to push the energy of the axial orbital *up* above $\varepsilon_F$ so that the Fermi surface has merely one sheet. The effective O $2p_z$ orbitals should therefore push the Ni $3d_{3z^2-1}$ level up as much as possible, and in order to accomplish this, the cation orbital should push the O $2p_z$ level down as little as possible. Hence, *a cation should be chosen whose covalent interaction with apical oxygen is as small as possible*. In this respect Sc is far better than Al, and among the possible insulators which are lattice matched with $LaNiO_3$, we have found $YScO_3$ and $PrScO_3$ to be the best. Habermeier has now been able to produce heterostructures of $PrNiO_3$ and $PrScO_3$, albeit not (yet) with $PrNiO_3$ monolayers. For $PrNiO_3/3(PrScO_3)$ we found the bottom of the $3z^2-1$ band to lie even a bit higher than for $LaNiO_3/YScO_3$, and the Wannier orbital calculated for this single conduction band is shown at the bottom left in Fig. 3. On the nickel atom at (0,0,0), this orbital has pure $x^2-y^2$ character, which antibonds to $x$ on the oxygens at $(\pm\frac{a}{2},0,0)$ and to $y$ on those at $(0,\pm\frac{a}{2},0)$. Each of these

4 oxygen orbitals bond to $3z^2-1$ on the nickels at $(\pm a,0,0)$ and $(0,\pm a,0)$, and the latter antibond perpendicular to the plane of the figure to $z$ on the apical oxygens at $\pm(\pm a,0,\sim\frac{c}{4})$ and $\pm(0,\pm a,\sim\frac{c}{4})$. The latter finally bond so weakly with the Sc $3z^2-1$ orbitals at $\pm(\pm a,0,\frac{c}{2})$ and $\pm(0,\pm a,\frac{c}{2})$, that this is cannot be seen in the figure.

We now compare with the cuprates. They have configuration $d^9$ with the $x^2-y^2$ orbital half full and $3z^2-1$ full, so that there is *no pd* bond between Cu and apical oxygen, which is therefore far away. In this case, the axial orbital is Cu $4s$ antibonding to the two neighboring apical-oxygen $2p_z$ orbitals, each of which bond to their neighbor cation axial orbital, e.g., La $3z^2-1$, and antibond to Cu $3z^2-1$. For the cuprates it has been found, but not understood, that the closer the calculated energy of the axial orbital is above $\varepsilon_F$, the higher is the measured $T_{c\,max}$ [3]. Now, in this case one wants to minimize the pushing up of the Cu $4s$ level by the apical-oxygen $2p_z$ orbital, and that happens when the distance to apical oxygen is large, as in $HgBa_2CuO_4$. The axial level can however not lie lower than the pure Cu $4s$ level, except in multi-layer cuprates ($HgBa_2Ca_2Cu_3O_8$), where this levels splits.

For such cuprates, the most bonding linear combination yields a Fermi surface sheet whose shape is almost as extreme as the one seen on the bottom right-hand side of Fig. 2. Increasing the number of $CuO_2$ layers beyond 3 has not lead to any increase of $T_{c\,max}$, probably because the interlayer coherence gets lost, but nickelate heterostructures point to another route: For those materials, the axial-orbital level approaches $\varepsilon_F$ from *below*, and the challenge is to shift it to slightly above $\varepsilon_F$. When this is done, the nickelate conduction band orbital is quite similar to that of the cuprate as shown at the bottom of Fig. 3.

In the calculations described so-far, all Ni atoms were forced to be equivalent, i.e., we did not allow for the *charge-* and *spin-density wave instabilities* common in *bulk* nickelates. Therefore, we have now performed LAPW GGA + $U$ calculations with larger cells for a number of nickelate heterostructures, as well as for $HgBa_2CuO_4$, searching for the leading instability as we increase the value of the on-site Coulomb interaction $U$ ($J=0.75$ eV). For the 90 K cuprate $HgBa_2CuO_4$, the leading instability is antiferromagnetism, as expected, and it occurs for $U\gtrsim 1$ eV. For $LaNiO_3/YScO_3$, the result is the same, thus boosting our hope that properly grown scandates will show superconductivity. For $LaNiO_3/LaAlO_3$, however, the leading instability, which sets in for $U\geq 4$ eV when $J=0.75$ eV, and earlier when $J=1$ eV, is to a magnetic, *charge disproportionated* ($2\,d^7 \longrightarrow d^6+d^8$) *insulator*. This is consistent with recent experiments [4].

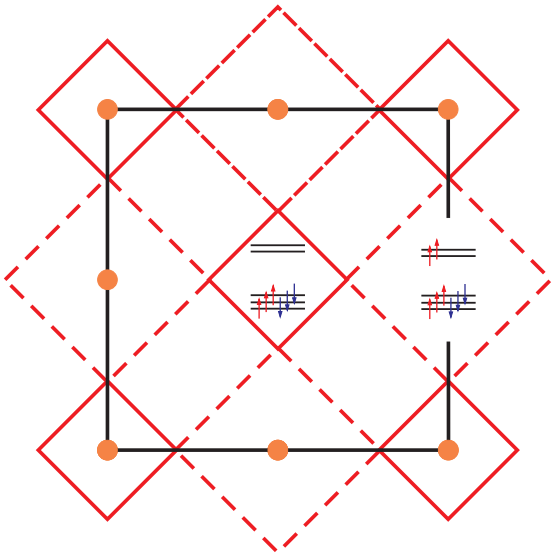

Figure 4: Schematic illustration of $2d^7 \rightarrow d^6+d^8$ charge disproportionation.

So we need to understand why the aluminate, but not the scandate, disproportionates. As illustrated in Fig. 4, charge disproportionation is a $\mathbf{q}=(1,1,0)\,\frac{\pi}{a}$ charge- and spin-density wave, in which the oxygen octahedra breathe alternatively in and out around Ni by approximately $\pm 4$ *pm*. Crudely speaking, the contracted sites have no $e_g$ electrons and the expanded sites have two, $d^{\uparrow}_{3z^2-1}$ and $d^{\uparrow}_{x^2-y^2}$. Such an instability is believed to be driven by the lattice and Hund's-rule couplings. Obviously, increasing the crystal-field splitting between the on-site energies of the $3z^2-1$ and $x^2-y^2$ Wannier orbitals makes charge disproportionation less favorable, and this is consistent with Fig. 2. The results of our calculations allow us to be more explicit: In the non-magnetic metallic state (Fig. 2), the lower and upper $e_g$ bands are separated for all $(k_x,k_y)$, except at one point, neglecting $k_z$, which is along the $k_x=k_y$ line (AZ) where the bands cannot hybridize. Charge disproportionation will now tend to gap *each* $e_g$

band around the lines bisecting the **q**-vectors, and in order that sufficient energy be gained, the result should be an insulator. This means that where the two bands come closest, i.e., along AZ, the two gaps should overlap. The gap required is thus larger than the separation between the $x^2-y^2$ and $3z^2-1$ bands *at* $\mathbf{k}=(\frac{1}{2},\frac{1}{2})\,\frac{\pi}{a}$, which is indicated by red stippled lines in Fig. 2. This is the crystal-field splitting relevant for charge disproportionation, and it is clearly much smaller for the aluminate than for the scandate. In the insulating, charge disproportionated state which our GGA + $U$ calculations find, the direct gap *is* between the two $e_g^{\uparrow}$ bands at $(\frac{1}{2},\frac{1}{2})\,\frac{\pi}{a}$, and is of size $\approx 0.7$ eV. In the $\downarrow$ channel, the gap is larger and is between the $t_{2g}$ and $e_g$ bands. Due to oxygen covalency, the magnetic moment is 1.5 rather than $2\,\mu_B$ on the expanded Ni site, and 0.5 rather than $0\,\mu_B$ on the contracted Ni site.

We thus predict that in order to produce metallic, and maybe even superconducting nickelate heterostructures, it is first of all essential that the $NiO_2$ layers be single and, secondly, that they be separated by an insulator whose cation counter to Ni interacts only weakly with apical oxygen, e.g., to use scandates instead of aluminates.

**References:**


[1] *Chaloupka, J. and G. Khaliullin.* Physical Review Letters **100**, 016404 (2008).

[2] *Hansmann, P., X. Yang, A. Toschi, G. Khaliullin, O.K. Andersen and K. Held.* Physical Review Letters **103**, 016401 (2009).

[3] *Pavarini, E., I. Dasgupta, T. Saha-Dasgupta, O. Jepsen and O.K. Andersen.* Physical Review Letters **87**, 047003 (2001).

[4] *Benckiser, E., M.W. Haverkort, S. Brück, E. Goering, S. Macke, A. Frañó, X. Yang, O.K. Andersen, G. Cristiani, H.-U. Habermeier, A.V. Boris, I. Zegkinoglou, P. Wochner, H.-J. Kim, V. Hinkov and B. Keimer.* Nature Materials **10**, 189–193 (2011).